J|A|C|S
ARTICLES
Published on Web 12/07/2002

Effects of Hydrogen Bonding on Metal Ion-Promoted Intramolecular Electron Transfer and Photoinduced Electron Transfer in a Ferrocene-Quinone Dyad with a Rigid Amide Spacer

Shunichi Fukuzumi,*,† Ken Okamoto,† Yutaka Yoshida,† Hiroshi Imahori,*,†,§ Yasuyuki Araki,‡ and Osamu Ito*,‡

Contribution from the Department of Material and Life Science, Graduate School of Engineering, Osaka University, CREST, Japan Science and Technology Corporation (JST), Suita, Osaka 565-0871, Japan, and Institute of Multidisciplinary Research for Advanced Materials, Tohoku University, CREST, Japan Science and Technology Corporation (JST), Sendai, Miyagi 980-8577, Japan

Received April 5, 2002; E-mail: fukuzumi@ap.chem.eng.osaka-u.ac.jp

Abstract: A ferrocene-quinone dyad (**Fc-Q**) with a rigid amide spacer and **Fc-(Me)Q** dyad, in which the amide proton acting as a hydrogen-bonding acceptor is replaced by the methyl group, are employed to examine the effects of hydrogen bonding on both the thermal and the photoinduced electron-transfer reactions. The hydrogen bonding of the semiquinone radical anion with the amide proton in **Fc-Q**$^{\bullet-}$ produced by the electron-transfer reduction of **Fc-Q** is indicated by the significant positive shift of the one-electron reduction potential of **Fc-Q**. The hyperfine coupling constants of **Fc-Q**$^{\bullet-}$ also indicate the existence of hydrogen bonding, agreeing with those predicted by the density functional calculation. The hydrogen-bonding dynamics in the photoinduced electron transfer from the ferrocene (Fc) to the quinone moiety (Q) in **Fc-Q** have been successfully detected in the femtosecond laser flash photolysis experiments. Thermal intramolecular electron transfer from Fc to Q in **Fc-Q** and **Fc-(Me)Q** also occurs efficiently in the presence of metal ions in acetonitrile at 298 K. The hydrogen bond formed between the semiquinone radical anion and the amide proton in **Fc-Q** results in remarkable acceleration of the rate of metal ion-promoted electron transfer as compared to the rate of **Fc-(Me)Q** in which hydrogen bonding is prohibited. The metal ion-promoted electron-transfer rates are well correlated with the binding energies of superoxide ion-metal ion complexes, which are derived from the g_{zz} values of the ESR spectra.

Introduction

Electron-transfer reactions are known to be regulated through noncovalent interactions such as hydrogen bonding which plays an important role in biological electron-transfer systems, where electron donors and acceptors are usually bound to proteins at a fixed distance.[1−5] Thus, electron-transfer reactions between donor and acceptor molecules bound to proteins have been studied extensively to understand the factors that control the electron-transfer processes.[6,7] A number of donor−acceptor linked systems with inert rigid spacers have also been developed to study the electron-transfer reactions between the donor and acceptor molecules at a fixed distance to understand the factors to control the electron-transfer process.[8−12] Because it would be impossible to connect donor and acceptor molecules if an electron transfer occurred thermally, photoexcitation of the donor

† Osaka University.
‡ Tohoku University.
§ Present address: Kyoto University.

(1) (a) Scheiner, S. *Hydrogen Bonding*; Oxford Press: Oxford, 1997. (b) Sessler, J. L.; Wang, B.; Springs, S. L.; Brown, C. T. In *Comprehensive Supramolecular Chemistry*; Murakami, Y., Ed.; Pergamon: New York, 1996; Vol. 4, pp 311−336. (c) Nocek, J. M.; Zhou, J. S.; Forest, S. D.; Priyadarshy, S.; Beratan, D. N.; Onuchic, J. N.; Hoffman, B. M. *Chem. Rev.* **1996**, *96*, 2459.
(2) (a) *The Photosynthetic Reaction Center*; Deisenhofer, J., Norris, J. R., Eds.; Academic Press: San Diego, 1993. (b) *Anoxygenic Photosynthetic Bacteria*; Blankenship, R. E., Madigan, M. T., Bauer, C. E., Eds.; Kluwer Academic Publishing: Dordrecht, 1995.
(3) (a) Niemz, A.; Rotello, V. M. *Acc. Chem. Res.* **1999**, *32*, 44. (b) Rotello, V. M. In *Electron Transfer in Chemistry*; Balzani, V., Ed.; Wiley-VCH: Weinheim, 2001; Vol. 4, pp 68−87.
(4) (a) Sessler, J. L.; Sathiosatham, M.; Brown, C. T.; Rhodes, T. A.; Wiederrecht, G. *J. Am. Chem. Soc.* **2001**, *123*, 3655. (b) De Rege, P. J. F.; Williams, S. A.; Therien, M. J. *Science* **1995**, *269*, 1409. (c) Myles, A. J.; Branda, N. R. *J. Am. Chem. Soc.* **2001**, *123*, 177.
(5) (a) Cukier, R. I.; Nocera, D. G. *Annu. Rev. Phys. Chem.* **1998**, *49*, 337. (b) Ghaddar, T. H.; Castner, E. W.; Isied, S. S. *J. Am. Chem. Soc.* **2000**, *122*, 1234.
(6) (a) McLendon, G.; Hake, R. *Chem. Rev.* **1992**, *92*, 481. (b) McLendon, G. *Acc. Chem. Res.* **1988**, *21*, 160. (c) Iseid, S. S.; Ogawa, M. Y.; Wishart, J. F. *Chem. Rev.* **1992**, *92*, 381.
(7) (a) Moser, C. C.; Keske, J. M.; Warncke, K.; Farid, R. S.; Dutton, P. L. *Nature* **1992**, *355*, 796. (b) Kirmaier, C.; Holton, D. In *The Photosynthetic Reaction Center*; Deisenhofer, J., Norris, J. R., Eds.; Academic Press: San Diego, 1993; Vol. II, pp 49−70. (c) Langen, R.; Chang, I.-J.; Germanas, J. P.; Richards, J. H.; Winkler, J. R.; Gray, H. B. *Science* **1995**, *268*, 1733. (d) Page, C. C.; Moser, C. C.; Chen, X.; Dutton, P. L. *Nature* **1999**, *402*, 47.
(8) (a) Gust, D.; Moore, T. A. In *The Porphyrin Handbook*; Kadish, K. M., Smith, K. M., Guilard, R., Eds.; Academic Press: San Diego, CA, 2000; Vol. 8, pp 153−190. (b) Gust, D.; Moore, T. A.; Moore, A. L. *Res. Chem. Intermed.* **1997**, *23*, 621. (c) Gust, D.; Moore, T. A.; Moore, A. L. *Acc. Chem. Res.* **1993**, *26*, 198. (d) Kurreck, H.; Huber, M. *Angew. Chem., Int. Ed. Engl.* **1995**, *34*, 849. (e) Gust, D.; Moore, T. A.; Moore, A. L. *Acc. Chem. Res.* **2001**, *34*, 40.

or acceptor moiety was required to start the electron-transfer reaction. As such, there has so far been no report on the effects of hydrogen bonding on thermal intramolecular electron-transfer reactions in donor−acceptor linked systems or on the hydrogen-bonding dynamics. However, the thermal electron-transfer reaction can be started by adding metal ions to the electron-transfer reaction system, which would otherwise show no reactivity.[13−16] Thus, the comparison of the metal ion-promoted electron-transfer rates of a donor−acceptor linked system involving hydrogen bonding and those without hydrogen bonding would provide quantitative insight into the actual role of hydrogen bonding in the thermal intramolecular electron-transfer reaction.

We report herein *thermal intramolecular* ET reactions of donor−acceptor linked systems with and without a hydrogen-bond acceptor, promoted by metal ions for the first time. A ferrocene-quinone dyad (**Fc-Q**) linked with an amide group and **Fc-(Me)Q** dyad, in which the amide proton acting as a hydrogen-bond acceptor is replaced by the methyl group, are employed to study the effects of hydrogen bonding between the carbonyl oxygen of the $Q^{\bullet-}$ moiety and N−H proton in the thermal and photoinduced electron-transfer reactions.[17] The hydrogen-bonding formation results in remarkable acceleration of the rate of metal ion-promoted electron transfer as compared to the rate of **Fc-(Me)Q** in which no hydrogen bond is formed. The successful detection of hydrogen-bonding dynamics in intramolecular photoinduced electron transfer in **Fc-Q** is also reported.

Experimental Section

General. ^{1}H NMR spectra were measured on a JEOL JNM-AL300 spectrometer. Fast atom bombardment mass spectra (FAB-MS) were obtained on a JEOL JMS-DX300 mass spectrometer. ESR spectra were recorded on a JEOL X-band spectrometer (JES-ME-1X) with a quartz ESR tube (1.2 mm i.d.).

Materials. Tris(2,2′-bipyridyl)ruthenium(III) hexafluorophosphate [$Ru(bpy)_3(PF_6)_3$] was prepared according to the literature.[18] Scandium triflate [$Sc(OTf)_3$ (99%, fw = 492.16)] was obtained from Pacific Metals Co., Ltd. (Taiheiyo Kinzoku). Lanthanum triflate [$La(OTf)_3$] was obtained from Aldrich as hexahydrate form. Yttrium triflate [$Y(OTf)_3$], europium triflate [$Eu(OTf)_3$], ytterbium triflate [$Yb(OTf)_3$], lutetium triflate [$Lu(OTf)_3$], and calcium triflate [$Ca(OTf)_2$] were prepared according to the literature.[19] Metal triflates were dried under vacuum evacuation at 403 K for 40 h prior to use. Magnesium perchlorate [$Mg(ClO_4)_2$] and barium perchlorate [$Ba(ClO_4)_2$] were obtained from Wako Pure Chemical Ind. Ltd., Japan. Chloroform-*d* was obtained from EURI SO-TOP, CEA, France.

Scheme 1

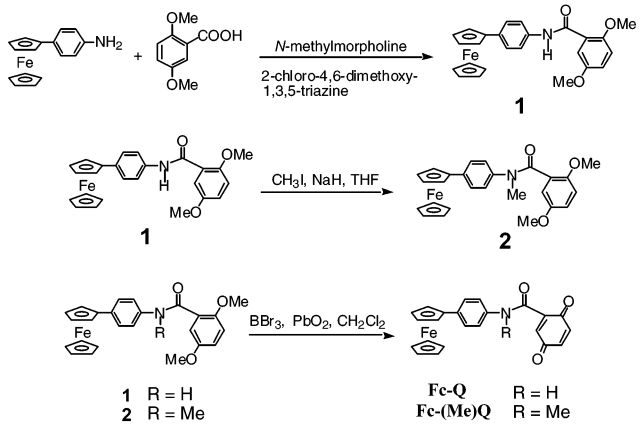

Synthesis. 4-Aminophenylferrocene was prepared according to the literature.[20] The synthetic route toward **Fc-Q** and **Fc-(Me)Q** is summarized in Scheme 1.

1: A solution of 2,5-dimethoxybenzoic acid (1.54 g, 8.5 mmol) and 2-chloro-4,6-dimethoxy-1,3,5-triazine (1.50 g, 8.5 mmol) in THF (40 mL) was stirred at room temperature for 1 h under nitrogen. *N*-Methylmorpholine (1.6 mL, 15 mmol) was then added dropwise at 0 °C. After the solution was stirred at 0 °C for 1 h, the solution was further stirred at room temperature for 1 h. After filtration of the mixture, the filtrate was added to a solution of 4-aminophenylferrocene (210 mg, 0.73 mmol) and *N*-methylmorpholine (1.0 mL, 9.1 mmol) in THF (10 mL). After the solution was stirred at 0 °C for 1 h, the solution was further stirred at room temperature for 4 h. After removal of solvent, the residue was purified by flash column chromatography (silica gel, chloroform). Subsequent recrystallization from ethanol gave **1** as an orange solid (280 mg, 0.63 mmol, 87%). ^{1}H NMR (300 MHz, $CDCl_3$): δ 9.92 (s, 1H(N−H)), 7.85 (d, 1H(Q), J = 2.9 Hz), 7.60 (d, 2H(Ph), J = 8.4 Hz), 7.47 (d, 2H(Ph), J = 8.4 Hz), 7.05 (dd, 1H(Q), J = 9.2, 3.1 Hz), 6.98 (d, 1H(Q), J = 9.0 Hz), 4.63 (t, 2H(Fc)), 4.30 (t, 2H(Fc)), 4.04 (s, 5H(Fc)), 4.03 (s, 3H(MeO)), 3.85 (s, 3H(MeO)). FABMS: *m*/*z* 441.

Fc-Q: A solution of **1** (885 mg, 2.0 mmol) in dichloromethane (60 mL) was stirred at 0 °C for 1 h under argon. A solution of boron tribromide (BBr_3) in the presence of oxygen and PbO_2 (1.5 g, 6.28 mmol) in dichloromethane (0.20 M, 25 mL) was then added dropwise at 0 °C. After the solution was stirred at 0 °C for 1 h, the solution was further stirred at room temperature for 3 h. Water and saturated aqueous sodium hydrogen carbonate were added to the solution. The organic phase was dried over sodium sulfate and filtrated. After removal of solvent, the residue was stirred in acetonitrile for 4 h, and the insoluble ingredient was recovered. Subsequent recrystallization from acetonitrile gave **Fc-Q** as a brown solid (20 mg, 0.29 mmol, 15%). ^{1}H NMR (300 MHz, $CDCl_3$): δ 10.30 (s, 1H(N−H)), 7.80 (s, 1H(Q)), 7.63 (d, 2H-(Ph), J = 8.6 Hz), 7.48 (d, 2H(Ph), J = 8.6 Hz), 6.90 (s, 2H(Q)), 4.64

(9) (a) Imahori, H.; Sakata, Y. *Adv. Mater.* **1997**, *9*, 537. (b) Imahori, H.; Sakata, Y. *Eur. J. Org. Chem.* **1999**, *2445*, 5. (c) Guldi, D. M. *Chem. Commun.* **2000**, 321. (d) Guldi, D. M.; Prato, M. *Acc. Chem. Res.* **2000**, *33*, 695. (e) Fukuzumi, S.; Imahori, H. In *Electron Transfer in Chemistry*; Balzani, V., Ed.; Wiley-VCH: Weinheim, 2001; Vol. 2, pp 927−975.
(10) (a) Wasielewski, M. R. In *Photoinduced Electron Transfer*; Fox, M. A., Chanon, M., Eds.; Elsevier: Amsterdam, 1988; Part A, p 161. (b) Wasielewski, M. R. *Chem. Rev.* **1992**, *92*, 435. (c) Jordan, K. D.; Paddon-Row, M. N. *Chem. Rev.* **1992**, *92*, 395.
(11) (a) Chambron, J.-C.; Chardon-Noblat, S.; Harriman, A.; Heitz, V.; Sauvage, J.-P. *Pure Appl. Chem.* **1993**, *65*, 2343. (b) Harriman, A.; Sauvage, J.-P. *Chem. Soc. Rev.* **1996**, *26*, 41. (c) Blanco, M.-J.; Jiménez, M. C.; Chambron, J.-C.; Heitz, V.; Linke, M.; Sauvage, J.-P. *Chem. Soc. Rev.* **1999**, *28*, 293. (d) Balzani, V.; Juris, A.; Venturi, M.; Campagna, S.; Serroni, S. *Chem. Rev.* **1996**, *96*, 759.
(12) (a) Maruyama, K.; Osuka, A.; Mataga, N. *Pure Appl. Chem.* **1994**, *66*, 867. (b) Osuka, A.; Mataga, N.; Okada, T. *Pure Appl. Chem.* **1997**, *69*, 797.
(13) (a) Fukuzumi, S.; Ohkubo, K. *Chem.-Eur. J.* **2000**, *6*, 4532. (b) Fukuzumi, S. *Bull. Chem. Soc. Jpn.* **1997**, *70*, 1. (c) Fukuzumi, S.; Itoh, S. In *Advances in Photochemistry*; Neckers, D. C., Volman, D. H., von Bünau, G., Eds.; Wiley: New York, 1998; Vol. 25, pp 107−172. (d) Fukuzumi, S. *Bull. Chem. Soc. Jpn.* **1997**, *70*, 1.
(14) Fukuzumi, S. In *Electron Transfer in Chemistry*; Balzani, V., Ed.; Wiley-VCH: Weinheim, 2001; Vol. 4, pp 3−67.
(15) (a) Fukuzumi, S.; Okamoto, T.; Otera, J. *J. Am. Chem. Soc.* **1994**, *116*, 5503. (b) Fukuzumi, S.; Inada, O.; Satoh, N.; Suenobu, T.; Imahori, H. *J. Am. Chem. Soc.* **2002**, *124*, 9181. (c) Fukuzumi, S.; Mori, H.; Imahori, H.; Suenobu, T.; Araki, Y.; Ito, O.; Kadish, K. M. *J. Am. Chem. Soc.* **2001**, *123*, 12458. (d) Fukuzumi, S.; Satoh, N.; Okamoto, T.; Yasui, K.; Suenobu, T.; Seko, Y.; Fujitsuka, M.; Ito, O. *J. Am. Chem. Soc.* **2001**, *123*, 7756.
(16) Fukuzumi, S.; Okamoto, K.; Imahori, H. *Angew. Chem., Int. Ed.* **2002**, *41*, 620.
(17) A preliminary report has appeared: Fukuzumi, S.; Yoshida, Y.; Okamoto, K.; Imahori, H.; Araki, Y.; Ito, O. *J. Am. Chem. Soc.* **2002**, *124*, 6794.
(18) DeSimone, R. E.; Drago, R. S. *J. Am. Chem. Soc.* **1970**, *92*, 2343.
(19) (a) Forsberg, J. H.; Spaziano, V. T.; Balasubramanian, T. M.; Liu, G. K.; Kinsley, S. A.; Duckworth, C. A.; Poteruca, J. J.; Brown, P. S.; Miller, J. L. *J. Org. Chem.* **1987**, *52*, 1017. (b) Kobayashi, S.; Hachiya, I. *J. Org. Chem.* **1994**, *59*, 3590.
(20) Imahori, H.; Tamaki, K.; Guldi, D. M.; Luo, C.; Fujitsuka, M.; Ito, O.; Sakata, Y.; Fukuzumi, S. *J. Am. Chem. Soc.* **2001**, *123*, 2607.

(t, 2H(Fc)), 4.33 (t, 2H(Fc)), 4.04 (s, 5H(Fc)). FAB-MS: *m*/*z* 411. TOF-MS: *m*/*z* 411. HR-MS (EI): *m*/*z* 411.0539 (Calcd for $C_{23}H_{17}NO_3Fe$ 411.0509). Anal. Calcd for $C_{23}H_{17}NO_3Fe \cdot 0.75H_2O$: C, 65.04; H, 4.39; N, 3.30. Found: C, 65.05; H, 4.40; N, 3.29.

Fc-(Me)Q: A solution of **1** (0.16 g, 0.36 mmol) in THF (30 mL) under nitrogen was treated sequentially with methyl iodide (65 μL, 1 mmol) and sodium hydride (65% oil dispersion, 0.015 g, 0.4 mmol) at room temperature. The reaction mixture was stirred at room temperature for 10 min (0 °C) and then was warmed at 60 °C under nitrogen for 1.5 h and again was stirred at room temperature for 2 h. After removal of solvent, subsequent recrystallization from ethanol gave **2** (Scheme 1). A solution of **2** and PbO_2 (1.5 g, 6.28 mmol) in dichloromethane (30 mL) was stirred at −78 °C under oxygen. A solution of boron tribromide (BBr_3) in dichloromethane (5 mmol, 5 mL) was then added dropwise at −78 °C. After the solution was stirred at −78 °C for 10 min, the solution was further stirred at room temperature overnight. Water and saturated aqueous sodium hydrogen carbonate were added to the solution. The organic phase was dried over sodium sulfate and filtrated. After removal of solvent, subsequent recrystallization from chloroform and hexane gave **Fc-(Me)Q** as a brown solid (42 mg, 0.10 mmol, 28%). ^{1}H NMR (300 MHz, $CDCl_3$): δ 7.4 (d, 2H(Ph), J = 9 Hz), 6.9 (d, 2H(Ph), J = 9 Hz), 6.54 (m, 1H(Q)), 6.51 (m, 2H(Q)), 4.5 (t, 2H(Fc), J = 2 Hz), 4.3 (t, 2H(Fc), J = 2 Hz), 3.9 (s, 5H(Fc)), 3.4 (s, 3H(N−Me)). FAB-MS: *m*/*z* 427 (+2H$^+$). TOF-MS: *m*/*z* 427 (+2H$^+$). HR-MS (EI): *m*/*z* 425.0705 (Calcd for $C_{24}H_{19}NO_3Fe$ 425.0666).

X-ray Structure Determination. Fc-Q was dissolved in chloroform containing a little acetonitrile and recrystallized under an atmospheric pressure of diethyl ether vapor. Data of X-ray diffraction were collected by a Rigaku RAXIS-RAPID imaging plate two-dimensional area detector using graphite-monochromated Mo Kα radiation (λ = 0.71069 Å) to 2θ max of 55.0°. All of the crystallographic calculations were performed by using the teXsan software package of the Molecular Structure Corp. [teXsan: Crystal Structure Analysis Package, Molecular Structure Corp. (1985 and 1999)]. The crystal structure was solved by direct methods and refined by full-matrix least squares. All non-hydrogen atoms and hydrogen atoms were refined anisotropically and isotropically, respectively. A summary of the crystal data and experimental parameters for structure determinations is given in the Supporting Information (S1).

Spectral Measurements. The formation of **Fc$^+$-Q** was examined from the change in the UV−vis spectrum of **Fc-Q** (1.0×10^{-4} M) in the presence of Ru(bpy)$_3^{3+}$ by using a Hewlett-Packard 8453 diode array spectrophotometer with a quartz cuvette (path length = 10 mm) at 298 K. The formation of **Fc-Q$^{\bullet-}$** (**Fc-(Me)Q$^{\bullet-}$**) was examined by measuring the ESR spectrum of **Fc-Q** (**Fc-(Me)Q**) (1.0×10^{-4} M) in the presence of semiquinone radical anion (1.0×10^{-4} M) at 298 K. The g values and hyperfine coupling constants (hfc) were calibrated by using an Mn^{2+} marker. Tetramethylammonium hydroxide (TMAOH) was used for generation of the semiquinone radical anion in the reaction between hydroquinone and *p*-benzoquinone.[21] The formation of complexes of **Fc^{+-}Q$^{\bullet-}$** (**Fc$^+$-(Me)Q$^{\bullet-}$**) with each metal ion was examined by the change in the UV−vis spectrum of an acetonitrile solution of **Fc-Q** in the presence of each metal ion using a Hewlett-Packard 8453 diode array spectrophotometer and a Shimadzu UV-2200 spectrophotometer with a quartz cuvette (path length = 10 mm) at 298 K. The formation of complexes of **Fc^{+-}Q$^{\bullet-}$** with Mg^{2+} was also examined by measuring the ESR spectrum of an acetonitrile solution of **Fc-Q** in the presence of $Mg(ClO_4)_2$ at 298 K.

Kinetic Measurements. Kinetic measurements of *thermal intramolecular* electron-transfer reactions from the ferrocene moiety to the quinone moiety in **Fc-Q** in the presence of metal ions were performed on a UNISOKU RSP-601 stopped-flow rapid scan spectrophotometer with the MOS-type high sensitive photodiode array at various temperatures (258−298 K) using a Unisoku thermostated cell holder designed for low-temperature experiments. Typically, an acetonitrile solution of **Fc-Q** and $Mg(ClO_4)_2$ were transferred to the spectrophotometric cell. Rates of intramolecular electron-transfer reaction from the ferrocene moiety to the quinone moiety in the presence of metal ions were monitored by the rise of the absorption band at 800 nm due to the ferricenium ion moiety.

Electrochemical Measurement. Cyclic voltammetry (CV) measurements of **Fc-Q** were performed on a BAS 100W electrochemical analyzer in deaerated acetonitrile containing 0.1 M NBu_4PF_6 as supporting electrolyte at 298 K. A conventional three-electrode cell with a Pt working electrode (surface area of 0.3 mm^2) and a Pt wire as the counter electrode was utilized for the CV measurements. The Pt working electrode (BAS) was polished with a BAS polishing alumina suspension and rinsed with acetone before use. The measured potentials were recorded with respect to the $Ag/AgNO_3$ (0.01 M) reference electrode. The potential (vs Ag/Ag^+) was converted to values versus SCE by adding 0.29 V.[22]

Theoretical Calculations. Density functional (DFT) calculations were performed using the Amsterdam density functional (ADF) program version 1999.02 developed by Baerends et al.[23] with various basis sets on a COMPAQ DS20E computer. The gradient corrections of Becke88 (exchange) and Perdew86 (correlation) were included in the exchange-correlation functional. The hfc values are derived from multiplying 506.82 and spin density values of each hydrogen.

Time-Resolved Absorption Measurements. The picosecond laser flash photolysis was carried out using SHG (388 nm) of mode-locked Ti:sapphire laser (Clark-MXR, CPA-2001, fwhm of 150 fs) for an exciting source of Fc-Q or Fc-(Me)Q in benzonitrile (5×10^{-4} M) at 295 K. A white pulse generated by focusing the fundamental of the Ti:sapphire laser on a flowed D_2O/H_2O (1:1 volume) cell was used as a monitoring light. The monitoring light transmitted through a sample was detected with a Dual MOS detector (Hamamatsu Photonics C6140) equipped with a polychromator (Acton Research SpectraPro 150). The spectra were obtained by averaging 16 events on a microcomputer.

Results and Discussion

Structure of Fc-Q Dyad. Single crystals of **Fc-Q** were obtained by vapor diffusion of ether into an MeCN solution of **Fc-Q**. The crystallographic data are summarized in the Supporting Information (S1), and the ORTEP drawing is shown in Figure 1a. The selected bond distances and angles are also presented in the Supporting Information (S2). The closest distance between the quinone oxygen atom and the amide hydrogen is 2.17 Å, and the C−O bond lengths of two carbonyl groups of quinone are eventually the same (1.22 Å). These results indicate that there is no hydrogen bonding between the quinone oxygen atom and the amide proton in the neutral form.

Hydrogen-Bonding Formation upon Electron-Transfer Reduction. The cyclic voltammograms of **Fc-Q** exhibited two reversible one-electron redox couples of two redox active moieties at 0.39 and −0.16 V (vs SCE) as shown in Figure 2. The former one-electron redox potential corresponds to the Fc^+/Fc couple, which agrees with the one-electron oxidation potential of ferrocene (E_{ox}^0 = 0.37 V).[24] The latter potential thereby corresponds to the Q/Q$^{\bullet-}$ couple. The one-electron reduction potential of Q (E_{red}^0 = −0.16 V) is significantly shifted to a positive direction as compared to that of *p*-benzoquinone (−0.50 V) and more positive than the value of *p*-benzoquinone

(21) Fukuzumi, S.; Nakanishi, I.; Suenobu, T.; Kadish, K. M. *J. Am. Chem. Soc.* **1999**, *121*, 3468.

(22) Mann, C. K.; Barnes, K. K. *Electrochemical Reactions in Nonaqueous Systems*; Marcel Dekker: New York, 1990.

(23) (a) Baerends, E. J.; Ellis, D. E.; Ros, P. *Chem. Phys.* **1973**, *2*, 41. (b) Velde, G. T.; Baerends, E. J. *J. Comput. Phys.* **1992**, *99*, 84.

(24) Fukuzumi, S.; Mochizuki, S.; Tanaka, T. *Inorg. Chem.* **1989**, *28*, 2459.

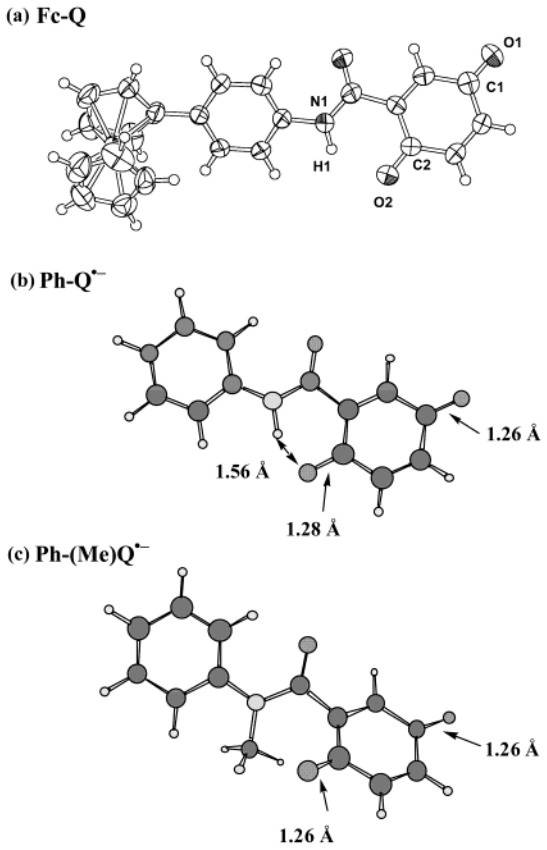

Figure 1. (a) ORTEP drawing of **Fc-Q**. (b) Optimized structure of Ph-Q•−. (c) Optimized structure of Ph-(Me)Q•−. The optimized structure is obtained by the ADF calculation with the V (small) basis set.[27]

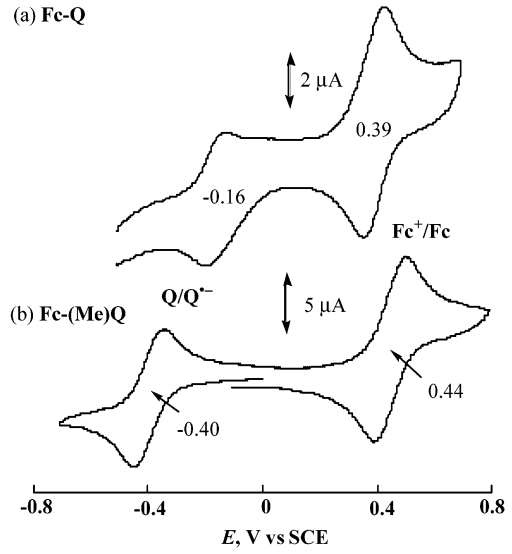

Figure 2. Cyclic voltammograms of (a) **Fc-Q** (0.5 mM) and (b) **Fc-(Me)Q** (0.5 mM) in MeCN containing 0.1 M Bu_4NPF_6.

possessing an electron-withdrawing substituent (−0.38 V for chloro-*p*-benzoquinone).[25] On the other hand, the cyclic voltammograms of **Fc-(Me)Q** (Figure 2b) exhibited two reversible one-electron redox couples of two redox active moieties at 0.44 and −0.40 V (vs SCE).[26] The E_{red}^0 value of Q (−0.40 V) in **Fc-(Me)Q** is significantly more negative as compared to that in **Fc-Q** (−0.16 V). Such a negative shift in the E_{red}^0 value of Q in **Fc-(Me)Q** as compared to that in **Fc-Q** indicates that the radical anion (Q•−) is stabilized by the hydrogen bond formed with the amide proton of the spacer.

The optimized geometry of Ph-Q•− in which Fc is omitted using the Amsterdam density functional (ADF) calculation with the V (small) basis set is shown in Figure 1b. The O−H distance between the quinone oxygen atom of Q•− and the amide hydrogen in Figure 1b is 1.56 Å, which is much shorter than the distance in the X-ray structure of neutral **Fc-Q** (Figure 1a).[27] This value is even shorter than the hydrogen-bonding distance between semiquinone radical anion and water (1.78 Å).[28] The C−O bond length of the hydrogen-bonded carbonyl group (1.28 Å) becomes longer than the bond length of the other carbonyl group (1.26 Å) due to the weakening of the C−O bond by the hydrogen bonding with the amide proton. For comparison, the optimized geometry of Ph-(Me)Q•− in which the N−H group is replaced by the N−Me group is shown in Figure 1c. There is no significant structural difference between Ph-Q•− and Ph-(Me)Q•− except for the absence of the hydrogen bond in the latter case.

To confirm the hydrogen-bonding formation of Q•− in the dyad, **Fc-Q•−** was produced by the electron-transfer reduction of **Fc-Q** by the semiquinone radical anion (see Experimental Section). Because the one-electron oxidation potential (E_{ox}^0) of the semiquinone radical anion, which is equivalent to the E_{red}^0 value of *p*-benzoquinone, is more negative than the E_{red}^0 value of Q in **Fc-Q**, an electron transfer from the semiquinone radical anion to Q in **Fc-Q** is thermodynamically feasible. In fact, an electron transfer from the semiquinone radical anion to Q occurs to produce **Fc-Q•−** (eq 1).

The ESR spectrum of **Fc-Q•−** thus produced is shown in Figure 3a together with the computer simulation spectrum (Figure 3b). The *g* value is determined as $g = 2.0055$, which is typical as the value of semiquinone radical anions.[29] The hyperfine coupling constants (hfc) are determined as 4.60 (1H), 2.05 (1H), and 1.75 G (1H). The hfc values obtained from the result in Figure 3b can be well reproduced by the ADF calculation with the V (small) basis set, which predicts the hfc values as 4.11 (1H), 2.18 (1H), and 1.57 G (1H).[30]

The radical anion (Q•−) in **Fc-(Me)Q•−** without hydrogen bonding is also produced by the electron-transfer reduction of **Fc-(Me)Q** by semiquinone radical anion as shown in Figure 3c. The hyperfine coupling (hfc) constants are determined by the computer simulation (Figure 3d) as 2.65 (1H), 2.25 (1H), and 2.20 G (1H), which are quite different from those observed in Fc-Q•− with hydrogen bonding. The hfc values can also be

(25) Fukuzumi, S.; Koumitsu, S.; Hironaka, K.; Tanaka, T. *J. Am. Chem. Soc.* **1987**, *109*, 305.

(26) The positive shift of the E_{red}^0 value of the quinone moiety of **Fc-(Me)Q** as compared to *p*-benzoquinone is ascribed to the electron-withdrawing effect of the carbonyl group in **Fc-(Me)Q**.

(27) Similar results were obtained using the B3LYP method. The ADF method with small V core gave the spin densities consistent with the experimentally determined hfc values in Figure 3b.

(28) O'Malley, P. J. *Phys. Chem. A* **1997**, *101*, 6334.

(29) Fukuzumi, S.; Nishizawa, N.; Tanaka, T. *J. Org. Chem.* **1984**, *49*, 3571.

(30) The hfc values were also calculated using the B3LYP method. Of all of the computational methods and basis sets tested, the ADF calculation with the V (small) set predicts the hfc values in closest agreement with experimental results in Figure 3 (see Supporting Information S3).

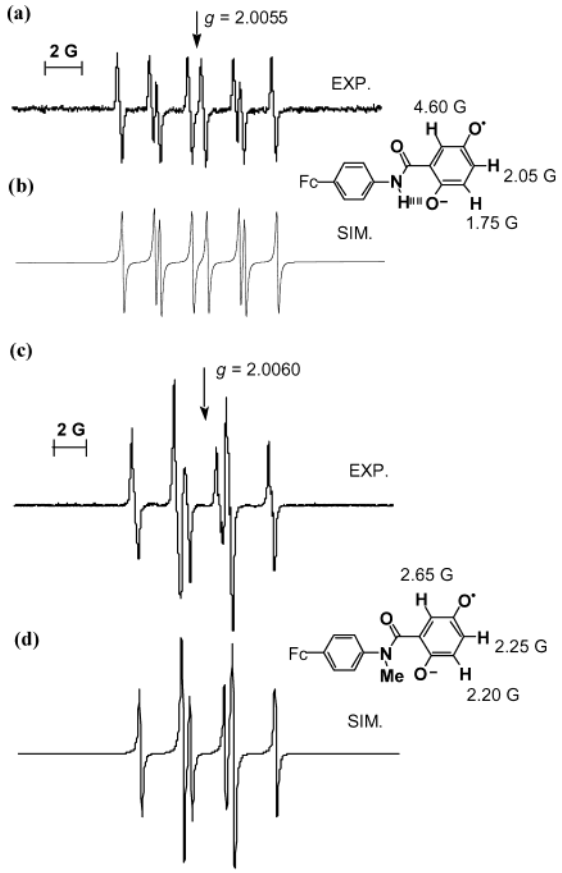

Figure 3. (a) ESR spectrum of **Fc-Q**$^{\bullet-}$ (1.0×10^{-4} M) in deaerated MeCN at 298 K and (b) the computer simulation spectrum. (c) ESR spectrum of **Fc-(Me)Q**$^{\bullet-}$ in deaerated MeCN at 298 K and (d) the computer simulation spectrum.

well reproduced by the ADF calculation, which predicts the hfc values as 3.19 (1H), 1.88 (1H), and 1.77 G (1H).[30]

Photoinduced Electron Transfer in Fc-Q. Photoexcitation of the Q moiety in **Fc-Q** in deaerated benzonitrile (PhCN)[31] with a 388 nm femtosecond (150 fs width) laser light results in the appearance of a new absorption band ($\lambda_{max} = 580$ nm) at 1 ns after the laser excitation as shown in Figure 4a. The absorption band at 580 nm is significantly red shifted as compared to the diagnostic absorption band of the semiquinone radical anion at 422 nm.[32] Such a red shift has been observed when the semiquinone radical anion is bound to a hard acid such as Mg^{2+}.[33] Thus, the absorption band at 580 nm may be assigned to Q$^{\bullet-}$, which is hydrogen bonded to the amide proton of the spacer. No such absorption band was observed in the case of **Fc-(Me)Q**, which has no hydrogen-bond acceptor. The absorption spectra of the hydrogen-bonded Q$^{\bullet-}$ in **Fc-Q**$^{\bullet-}$ and Q$^{\bullet-}$ without hydrogen bonding in **Fc(Me)Q**$^{\bullet-}$, produced by the electron-transfer reduction of **Fc-Q** and **Fc-(Me)Q**, are shown in Figure 4b.[34]

The absorption band at 450 nm due to Q$^{\bullet-}$ without hydrogen bonding appears immediately upon the laser excitation within

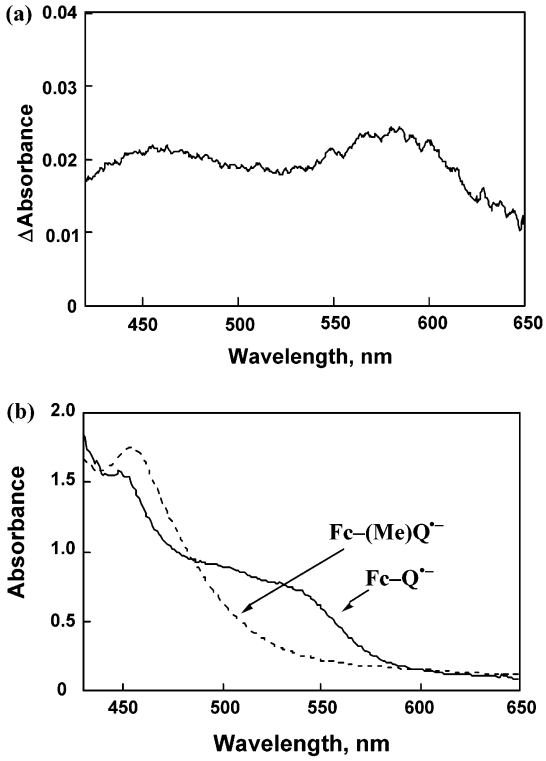

Figure 4. Time-resolved absorption spectrum of **Fc-Q** dyad (5.0×10^{-4} M) in argon-saturated PhCN excited at 388 nm (delay time: 1 ns) at 298 K. (b) Visible absorption spectra of **Fc-Q**$^{\bullet-}$ (0.40 mM, solid line) and **Fc-(Me)Q**$^{\bullet-}$ (0.40 mM, broken line) in deaerated MeCN at 298 K.

Scheme 2

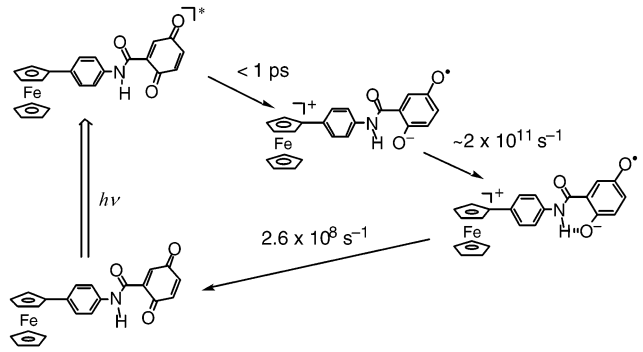

1 ps and decays with the first-order rate constant of $\sim 2 \times 10^{11}$ s^{-1} ($\tau \approx 5$ ps) to the residual absorbance, accompanied by the rise in absorption at 580 nm due to the hydrogen-bonded Q$^{\bullet-}$ (see Supporting Information S4).[35] The absorption at 580 nm decays at a longer time scale, obeying first-order kinetics with a rate constant of 2.6×10^8 s^{-1}. This indicates that electron transfer from Fc to the singlet excited state of Q occurs rapidly to produce **Fc-Q**$^{\bullet-}$ without changing the conformation (<1 ps), and then Q$^{\bullet-}$ forms the hydrogen bonding with the amide proton of the spacer ($\tau \approx 5$ ps), and the resulting radical ion pair decays via a back electron transfer to the ground state as shown in Scheme 2.

Metal Ion-Promoted Thermal Electron Transfer in Fc-Q and Fc-(Me)Q. No electron transfer from Fc to Q occurs in

(31) PhCN was used as a solvent for the laser flash photolysis, because good spectral resolution was obtained as compared to MeCN.
(32) Fukuzumi, S.; Nakanishi, I.; Maruta, J.; Yorisue, T.; Suenobu, T.; Itoh, S.; Arakawa, R.; Kadish, K. M. *J. Am. Chem. Soc.* **1998**, *120*, 6673.
(33) Fukuzumi, S.; Okamoto, T. *J. Am. Chem. Soc.* **1993**, *115*, 11600.
(34) The λ_{max} value of the hydrogen-bonded Q$^{\bullet-}$ varies slightly depending on the system: 580 nm for **Fc**$^{+}$**-Q**$^{\bullet-}$ (Figure 4a) and 550 nm for **Fc-Q**$^{\bullet-}$ (Figure 4b).
(35) The transient absorption due to the Fc^+ part which should be formed together with the Q$^{\bullet-}$ part is not detected probably because of the low extinction coefficient of Fc^+. This is confirmed by formation of Fc^+ ($\lambda_{max} = 800$ nm) by the chemical oxidation of **Fc-Q** with $[Ru(bpy)_3]^{3+}$ (bpy = 2,2′-bipyridine).

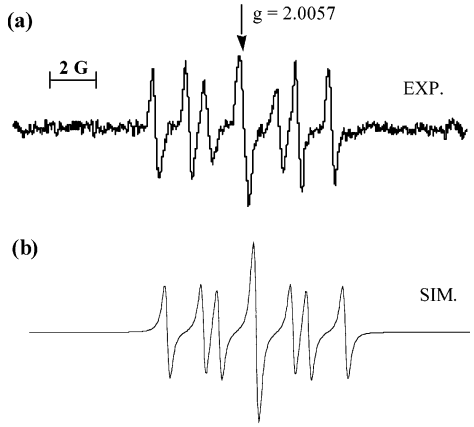

Figure 5. (a) ESR spectrum of $\mathbf{Fc}^{+}$-$\mathbf{Q}^{\bullet-}$ (4.0×10^{-4} M) in the presence of Mg^{2+} (7.5×10^{-2} M) in deaerated MeCN at 298 K and (b) the computer simulation spectrum.

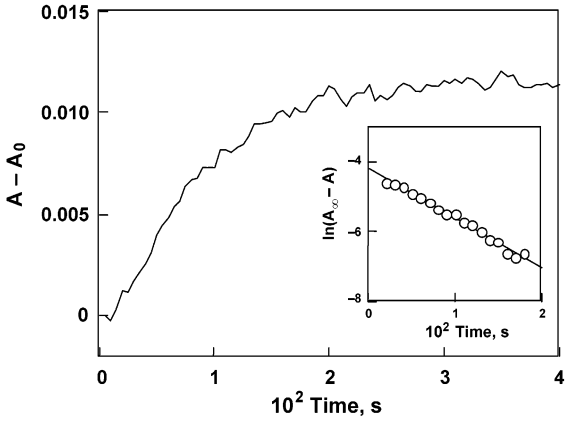

Figure 6. Time course of the absorption change at 800 nm due to formation of $\mathbf{Fc}^{+}$-$\mathbf{Q}^{\bullet-}$ by the intramolecular electron transfer in **Fc-Q** (1.0×10^{-4} M) in the presence of $Mg(ClO_4)_2$ (0.10 M) in deaerated MeCN at 298 K. Inset: First-order plot.

Scheme 3

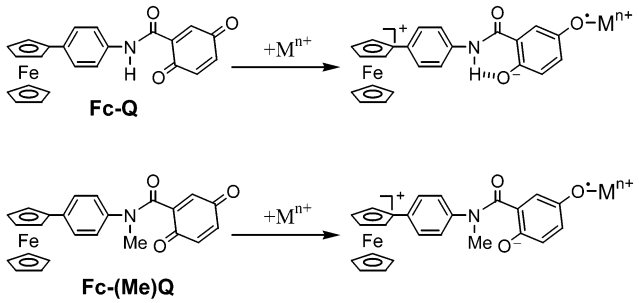

Fc-Q thermally in MeCN at 298 K. However, addition of Mg^{2+} (0.10 M) results in formation of Fc^{+} as indicated by the appearance of the absorption band due to Fc^{+} at 800 nm together with the absorption band at 420 nm (see Supporting Information S5). The absorption band at 420 nm which may be assigned to $Q^{\bullet-}$ bound to Mg^{2+} is blue shifted as compared to those of non-hydrogen-bonded $Q^{\bullet-}$ (450 nm) and hydrogen-bonded $Q^{\bullet-}$ (580 nm). Such a significant blue shift has indeed been observed when $Q^{\bullet-}$ is bound to two Mg^{2+} ions: the absorption maximum of the $Q^{\bullet-}$-Mg^{2+} complex (590 nm) is blue shifted to 410 nm for $Q^{\bullet-}$-$2Mg^{2+}$.[33]

To confirm the formation of a paramagnetic species, that is, $Q^{\bullet-}$ bound to both Mg^{2+} and the amide proton, the ESR spectrum was measured after addition of Mg^{2+} ion (7.5×10^{-2} M) to an MeCN solution of **Fc-Q** (4.0×10^{-4} M). The observed ESR spectrum is shown in Figure 5a together with the computer simulation spectrum (Figure 5b). The hyperfine coupling (hfc) constants are determined as 3.95 (1H), 2.30 (1H), and 1.60 G (1H). The hfc values are similar to those observed for the hydrogen-bonded $Q^{\bullet-}$ in $\mathbf{Fc\text{-}Q}^{\bullet-}$ without Mg^{2+} ion in Figure 3b. However, the largest hfc value (3.95 G) is significantly smaller than the value without Mg^{2+} ion (4.60 G) due to the spin delocalization to the Mg nucleus. The g value is determined as $g = 2.0057$, which is slightly larger than the value of $\mathbf{Fc\text{-}Q}^{\bullet-}$ without Mg^{2+} ion.

The rate of formation of Fc^{+} monitored by the appearance of the absorption band at 800 nm obeys first-order kinetics as shown in Figure 6. The appearance and the observed-first-order rate constant (k_{obs}) increase linearly with increasing Mg^{2+} concentration (Supporting Information S6). The second-order rate constant (k_{et}) is determined from the slope of the linear plot of k_{obs} versus $[Mg^{2+}]$ as 1.4×10^{3} M^{-1} s^{-1}. When **Fc-Q** is replaced by **Fc-(Me)Q** which contains no hydrogen-bond acceptor, the k_{et} value (0.4 M^{-1} s^{-1}) is much smaller than the k_{et} value (1.4×10^{3} M^{-1} s^{-1}) of the electron transfer in **Fc-Q**, which is promoted not only by Mg^{2+} but also by the hydrogen bond formed between the $Q^{\bullet-}$ moiety and the amide proton.

A variety of metal ions (M^{n+}: triflate salts) were employed to promote the intramolecular electron transfer in **Fc-Q** and **Fc-(Me)Q** (Scheme 3). The k_{et} values are determined as listed in Table 1.[30] The promoting effects of metal ions vary significantly depending on the Lewis acidity of metal ions. We have recently reported that the binding energies (ΔE) of metal ions

Table 1. Electron-Transfer Rate Constants (k_{et}) of M^{n+}-Promoted Electron Transfer in **Fc-Q** and **Fc-(Me)Q** in Deaerated MeCN at 298 K

	k_{et}, $M^{-1}s^{-1}$	
M^{n+}	Fc-Q	Fc-(Me)Q
Sc^{3+}	1.0×10^{9}	2.0×10^{5}
Y^{3+}	2.5×10^{6}	3.8×10^{2}
La^{3+}	1.0×10^{6}	4.0×10^{1}
Eu^{3+}	7.0×10^{5}	1.0×10^{2}
Yb^{3+}	1.8×10^{5}	2.3×10^{2}
Lu^{3+}	2.0×10^{5}	9.4×10^{1}
Mg^{2+}	1.4×10^{3}	0.4
Ca^{2+}	5.0	*a*
Ba^{2+}	0.9	*a*

[a] Not determined.

with $O_2^{\bullet-}$ can be evaluated from the g_{zz} values of the $O_2^{\bullet-}$-M^{n+} complexes and that the ΔE values are well correlated with the promoting effects of metal ions in intermolecular electron-transfer reduction of *p*-benzoquinone as well as O_2.[13a] Figure 7 shows plots of log k_{et} versus ΔE for the M^{n+}-promoted intramolecular electron transfer in **Fc-Q** and **Fc-(Me)Q**. The k_{et} value of the Sc^{3+}-promoted electron transfer in **Fc-Q** is the largest among metal ions investigated, and this is 10^4 times larger than the corresponding k_{et} value of **Fc-(Me)Q**.[36] The log k_{et} values of M^{n+}-promoted electron transfer in **Fc-Q** are linearly correlated with the ΔE values, and each value is ca. 10^4 times larger than the k_{et} values of **Fc-(Me)Q**. The stabilization of the $Q^{\bullet-}$ moiety by hydrogen bonding with the amide proton in $\mathbf{Fc\text{-}Q}^{\bullet-}$ results in the positive shift in E_{red}^{0} of **Fc-Q** as compared

(36) In the case of **Fe-(Me)Q**, no electron transfer occurred when a weaker Lewis acid than Mg^{2+} such as Ca^{2+} or Ba^{2+} was employed.

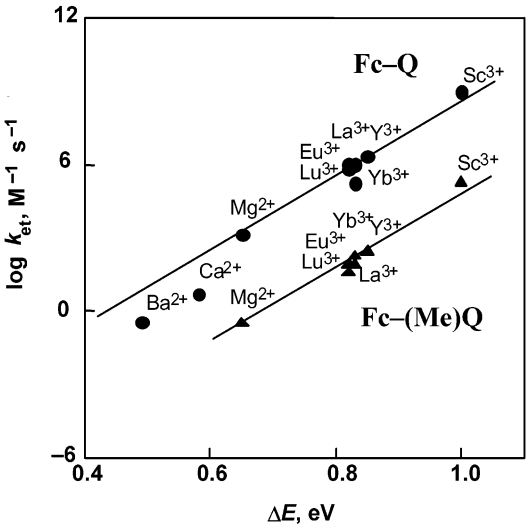

Figure 7. Plots of log k_{et} versus ΔE in M^{n+}-promoted electron transfer in **Fc-Q** and **Fc-(Me)Q** in MeCN at 298 K.

to that of **Fc-(Me)Q** in which the amide proton is replaced by the methyl group. The 10^4 times difference in the k_{et} values corresponds to the difference in the one-electron reduction potential between **Fc-Q** (E_{red}^0 vs SCE = −0.16 V) and **Fc-(Me)Q** (E_{red}^0 vs SCE = −0.40 V), because the ratio of the rate constant is given by exp(0.24 (eV)/k_BT), which is equal to 1.1×10^4 at 298 K (k_B is the Boltzmann constant). Thus, the remarkable difference in the k_{et} values between **Fc-Q** and **Fc-(Me)Q** is ascribed to the effect of hydrogen bonding formed between the $Q^{\bullet-}$ moiety and the amide proton in $\mathbf{Fc}^+$-$\mathbf{Q}^{\bullet-}$.[37]

In conclusion, the present study has demonstrated that formation of hydrogen bonding between the $Q^{\bullet-}$ moiety and the amide proton results in remarkable acceleration of the rate of metal ion-promoted intramolecular electron transfer from Fc to Q in **Fc-Q**. The hydrogen-bonding formation is coupled with the metal ion-promoted thermal electron-transfer reaction in **Fc-Q**. In contrast, photoexcitation of **Fc-Q** results in electron transfer from Fc to the singlet excited state of Q to produce $\mathbf{Fc\text{-}Q}^{\bullet-}$ without changing the conformation (<1 ps), and then $Q^{\bullet-}$ forms the hydrogen bonding with the amide proton of the spacer ($\tau \approx 5$ ps).

Acknowledgment. This work was partially supported by a Grant-in-Aid for Scientific Research Priority Area (No. 11228205) from the Ministry of Education, Culture Sports, Science, and Technology, Japan.

Note Added after ASAP: The ASAP version of this paper published 12/7/2002 on the Web did not show the cation on the ferrocene moieties after addition of the metal ions in Scheme 3. The final Web version published 12/30/2002 and the print version are correct.

Supporting Information Available: X-ray crystallographic data (S1), selected bond lengths of **Fc-Q** (S2), comparison of calculation methods of the hfc values (S3), time profile of photoinduced electron transfer in **Fc-Q** (S4), Mg^{2+}-promoted electron transfer in **Fc-Q** (S5), and plot of k_{obs} versus [Mg^{2+}] (S6) (PDF). This material is available free of charge via the Internet at http://pubs.acs.org.

JA026441V

(37) There is some structural difference between $Ph\text{-}Q^{\bullet-}$ (Figure 1b) and $Ph\text{-}(Me)Q^{\bullet-}$ (Figure 1c), which may also affect the rate of metal ion-promoted electron transfer of **Fc-Q** and **Fc-(Me)Q** in addition to the effect of hydrogen bond.